VOL. 21, NO. 2, 2022, 90-94
www.elektrika.utm.my
ISSN 0128-4428

ELEKTRIKA
Journal of Electrical Engineering

Single-coil Design Approach for Dual-band Near-field Coupled Resonators

Lai Ly Pon

Southern University College,
Malaysia

Corresponding author: llpon@sc.edu.my

Abstract: With the adoption of single coil approach, printed spiral resonator design strategy for near-field wireless energy transfer is presented. A pair of symmetrical resonators operating at high frequency band specifically 6.78 MHz and 13.56 MHz is designed. Simulated power transfer efficiency (PTE) of over 88% are obtained for both frequencies when coupled spiral resonators separated at a distance of 25 mm is integrated with hybrid compensation network topology. The variance of PTE between both frequencies is about 0.04.

Keywords: impedance matching, power transfer efficiency, printed spiral resonator, single-coil, wireless energy transfer.

Article History: received 12 December 2021; accepted 1 August 2022; published 25 August 2022.

1. INTRODUCTION

Near field wireless energy transfer system operating at more than one frequency band exceed its single band predecessor by offering the prospect of simultaneous energy and data transfer as well as dual-mode energy transfer functionalities. One of the commonly used performance metrics in wireless energy transfer is power transfer efficiency (PTE). There is a tendency that PTE for either one of the concerned frequencies greatly exceed the other. On the other hand, this shortcoming will be ideal for simultaneous energy and data functionalities provided that maximum transfer efficiency and sufficient bandwidth allocation are not compromised.

Multi-coil [1], [2], [3] and single-coil [4], [5], [6] design approaches are used to achieve the aforementioned intentions. Nevertheless, similar with any front-end designs, both methods come with their respective downsides. Designing separate resonators as in the case of multi-coil approach often viewed as a better option since stand-alone resonators with its corresponding impedance matching networks is capable of realizing highest transfer efficiency as demonstrated in [7] with the implementation of two circular defected ground structure (DGS). Even though DGS offers miniaturized design, the lowest resonance frequency to date is 280 MHz [8].

Hence, this paper presents a design approach for a dual-band printed spiral resonator with two resonant frequencies at f_1, 6.78 MHz and f_2, 13.56 MHz with the aim of accomplishing minimum transfer efficiency variance between first and second resonant frequency. This paper is organized as follows. Section 2 presents the design method while Section 3 discusses results obtained. A comparison between proposed design in this work and other published work is presented. Finally, this paper is concluded in Section 4.

2. DESIGN METHOD

There are two predominant stages in the front-end design of wireless energy transfer system namely resonator design and impedance transformation network. Full-wave electromagnetic simulator, CST Microwave Studio is employed in the design of spiral resonator. Design and enhancement steps are portrayed in Figure 1. Selection of optimal axial distance, z_{OP} is equally important in order to extract maximum magnetic field excitation [9], [10]. The optimal axial distance is found by

$$z_{OP} = 0.3931\, d_o \tag{1}$$

where d_0 is outermost diameter length of loop. Since calculated optimal distance is 23.6 mm, 25 mm is selected before performing any optimization.

Geometrical constraints specified are number of turns, width and spacing of conductive trace. Dimension of the proposed double-sided design is 70 mm by 75 mm with FR-4 substrate thickness of 1.6 mm. Conductor thickness opted is 0.07 mm. Thicker conductor will aid in the reduction of resistance. A total of seven turns are designed with three and four loops etched on top and bottom layer of the substrate respectively. Optimization is performed to enhance geometrical layout as this remains as one of essential rectification techniques for dual-band resonator designs [11]. Other parameter properties are detailed in Table 1 while the proposed design layout is depicted in Figure 2.

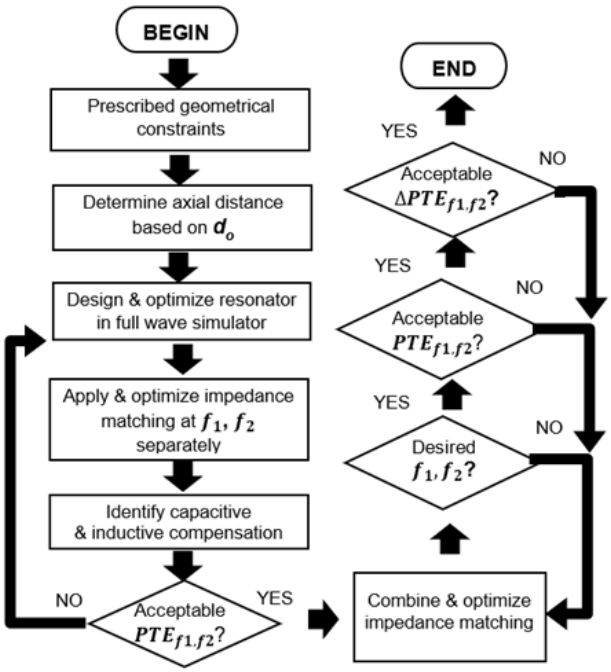

Figure 1. Single coil approach design strategy

Table 1. Parameters of resonator design

Symbols	Parameters	Value (mm)
d_o	Outermost side length	60
d_i	Innermost side length	10.35
w_{ot}	Outermost conductor width top layer	2.5
w_{it}	Innermost conductor width top layer	1.3
s_{ot}	Outermost spacing top layer	4.6
s_{it}	Innermost spacing top layer	6.9
w_{ob}	Outermost conductor width bottom layer	2.5
w_{ib}	Innermost conductor width bottom layer	1.25
s_{ob}	Outermost spacing bottom layer	3.475
s_{ib}	Innermost spacing bottom layer	8.3

Following geometrical layout refinement on resonator design, the subsequent steps involve impedance matching. Simultaneous conjugate matching is critical in ensuring maximum power transfer between a pair of coupled resonators [12]. There are numerous ways to implement impedance matching using lumped elements as reactive compensation. Single capacitive compensation, C_n can be derived from equation (2) where f_r and L denote desired resonance frequency and loop inductance.

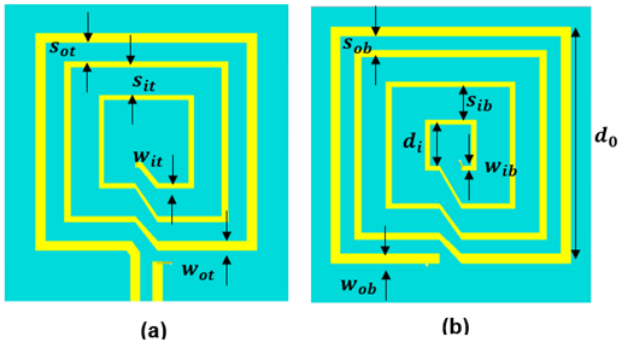

Figure 2. Single coil approach design layout: a) Top view, b) Bottom view

$$C_n = ((2\pi f_r)^2 L)^{-1} \quad (2)$$

Double capacitive compensation can be achieved by connecting a series and parallel capacitors at the transmitting and receiving resonators. As shown in Figure 3, this compensation network topology is also commonly known as L-matching. Capacitive values can be determined from inbuilt search algorithm available in full wave finite element simulator.

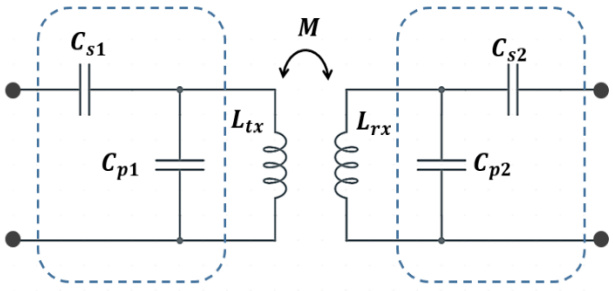

Figure 3. Equivalent schematic of double capacitive compensation

Apart from double capacitive compensation, parallel resonant circuit is applied in order to realize peak transfer efficiency at dual resonance frequency. Both parallel resonant $L-C$ tank and series resonant $L-C$ branch have been implemented in [13]. However, there is a considerable variance of transfer efficiency between lower and higher resonance frequency. In this design, parallel resonant circuit and double capacitive compensation are proposed. Table 2 lists the separate initial and optimized values of reactive components. Figure 4 depicts equivalent schematic of proposed design. Optimization is performed after combining both impedance matching methods. The initial and optimized values of reactive components are shown in Table 3.

Table 2. Separate initial and optimized impedance matching

Resonance Frequency	Parameters	Initial	Optimized
f_1	C_{s1}	27 pF	158.57 pF
	C_{p1}	252 pF	132.48 pF
f_2	L_1	2.14 µH	3.65 µH
	C_1	64.36 pF	101.57 pF

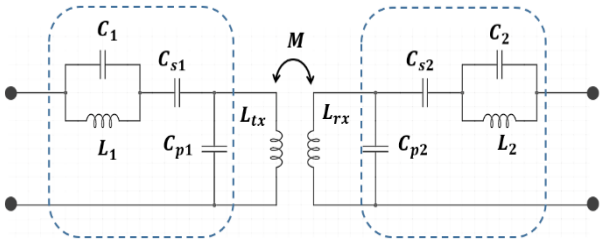

Figure 4. Equivalent schematic of proposed design

Table 3. Combined initial and optimized impedance matching

Parameters	Initial	Optimized
L_1	3.65 µH	1.86 µH
C_1	101.57 pF	31.64 pF
C_{s1}	158.57 pF	87.21 pF
C_{p1}	132.48 pF	146.96 pF
L_2	3.65 µH	2.69 µH
C_2	101.57 pF	25.24 pF
C_{s2}	158.57 pF	87.70 pF
C_{p2}	132.48 pF	102.06 pF

3. RESULT AND DISCUSSION

Performance of wireless energy transfer link can be evaluated through *S*-parameters. Figure 5 shows simulated input reflection coefficient, S_{11} and transmission coefficient, S_{21}. Two resonances are achieved at targeted frequencies, 6.78 MHz and 13.56 MHz. Power transfer efficiency is derived from the magnitude of transmission coefficient, S_{21} as given by Equation (3) [14].

$$PTE\ (\%) = 100(|S_{21}|^2) \quad (3)$$

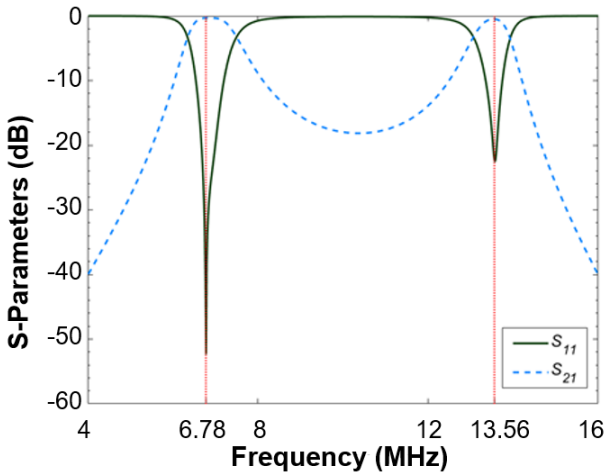

Figure 5. Simulated S-parameters plot of single coil design approach for dual-band near-field coupled resonators

As shown in Figure 6, PTE obtained at 6.78 MHz and 13.56 MHz are 93% and 89 % respectively. The average transfer efficiency computed is 91%. Equation (4) is employed to compute the difference between transfer efficiency at each targeted resonance frequency which is represented by $\Delta PTE_{f1,f2}$. Table IV lists the computed average and variance of transfer efficiency. Result obtained indicates that single coil-approach integrated with hybrid compensation network topology is possible in decreasing the gap between PTE of first resonance and second resonance frequency. Another advantage of employing single-coil approach besides intercoupling decrement [13] is geometrical area reduction. Table V summarizes comparison with other published works.

$$\Delta PTE_{f1,f2} = |PTE_{f1} - PTE_{f2}| \quad (4)$$

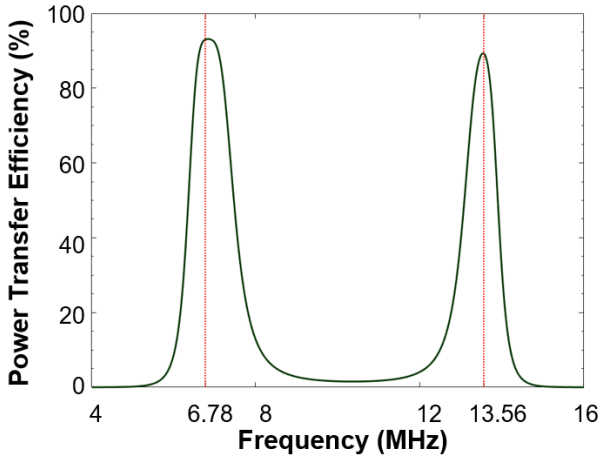

Figure 6. Simulated PTE at fixed axial distance of 25 mm

Table 4. Simulated Power Transfer Efficiency

d (mm)	PTE_{f1} (%)	PTE_{f2} (%)	PTE_{av} (%)	$\Delta PTE_{f1,f2}$
25	93	89	91	0.04

Table 5. Comparison with other published works

Ref	Approach	f_1	f_2	PTE_{f1} (%)	PTE_{f2} (%)	PTE_{av} (%)	Variance, $\Delta PTE_{f1,f2}$	z (mm)	TX size (mm^2)	Link	Impedance Matching
[2]	Multi-coil	200 kHz	6.78 MHz	70.6	78	74.3	0.07	25	11125	Asymmetrical	Hybrid compensation
[15]	Multi-coil	6.78 MHz	13.56 MHz	72.34	74.02	73.18	0.02	30	7200	Symmetrical	Capacitive compensation
[8]	Multi-coil	280 MHz	490 MHz	91.2	79.4	85.3	0.12	6	400	Symmetrical	Capacitive compensation
[4]	Single-coil	200 kHz	6.78 MHz	55	74	64.5	0.19	50	10350	Asymmetrical	Hybrid compensation
[5]	Single-coil	6.78 MHz	13.56 MHz	49.14	37.21	43.175	0.12	200	19200	Asymmetrical	Coupling loop and capacitive compensation
This work	Single-coil	6.78 MHz	13.56 MHz	93	89	91	0.04	25	5250	Symmetrical	Hybrid compensation

4. CONCLUSION

This paper is intended to serve as a simplified design guideline for near-field coupled resonators using single-coil approach. Targeted dual resonance frequency with minimal variation ratio of 0.04 between each transfer efficiency is accomplished with integration of hybrid compensation network topology acquired based on numerical simulation. Single-coil approach proposed is indicative that dual-mode resonator implementation is viable without necessitating additional structures such as two standalone resonators or repeaters.

REFERENCES

[1] W. Lee and D. Ahn, "Wireless power transfer under wide distance variation using dual impedance frequency," *Electron.*, vol. 9, no. 1, 2020, doi: 10.3390/electronics9010110.

[2] D. Ahn and P. P. Mercier, "Wireless Power Transfer With Concurrent 200-kHz and 6.78-MHz Operation in a Single-Transmitter Device," *IEEE Trans. POWER Electron. VOL. 31, NO. 7, JULY 2016*, vol. 31, no. 7, pp. 5018–5029, 2016.

[3] D. Kwon, T. D. Yeo, K. S. Oh, J. W. Yu, and W. S. Lee, "Dual Resonance Frequency Selective Loop of Near-Field Wireless Charging and Communications Systems for Portable Device," *IEEE Microw. Wirel. Components Lett.*, vol. 25, no. 9, pp. 624–626, 2015, doi: 10.1109/LMWC.2015.2451352.

[4] M.-L. Kung and K.-H. Lin, "Dual-Band Coil Module With Repeaters for Diverse Wireless Power Transfer Applications," *IEEE Trans. Microw. Theory Tech.*, vol. 66, no. 1, pp. 332–345, Jan. 2018, doi: 10.1109/TMTT.2017.2711010.

[5] K. Ding, Y. Yu, and H. Lin, "A Novel Dual-Band Scheme for Magnetic Resonant Wireless Power Transfer," Prog. Electromagn. Res. Lett., vol. 80, no. August, pp. 53–59, 2018, doi: 10.258/ PIERL18082201.

[6] K. Furusato, T. Imura, and Y. Hori, "Multi-band Coil Design for Wireless Power Transfer at 85 kHz and 6.78 MHz Using High Order Resonant Frequency of Short End Coil," *2016 Int. Symp. Antennas Propag.*, pp. 50–51, 2016.

[7] F. Tahar, A. Barakat, R. Saad, K. Yoshitomi, and R. K. Pokharel, "Dual-Band Defected Ground Structures Wireless Power Transfer System With Independent External and Inter-Resonator Coupling," *IEEE Trans. Circuits Syst. II Express Briefs*, vol. 64, no. 12, pp. 1372–1376, Dec. 2017, doi: 10.1109/TCSII.2017.2740401.

[8] H. A. Atallah, R. Hussein, and A. B. Abdel-Rahman, "Compact coupled resonators for small size dual-frequency wireless power transfer (DFWPT) systems," *IET Microwaves, Antennas Propag.*, vol. 14, no. 7, pp. 617–628, 2020, doi: 10.1049/iet-map.2018.5693.

[9] A. A. Eteng, S. K. Abdul Rahim, and C. Y. Leow, "Geometrical Enhancement of Planar Loop Antennas for Inductive Near-Field Data Links," *IEEE Antennas Wirel. Propag. Lett.*, vol. 14, pp. 1762–1765, 2015, doi: 10.1109/LAWP.2015.2423276.

[10] A. A. Eteng, S. K. Abdul Rahim, C. Y. Leow, B. W. Chew, and G. A. E. Vandenbosch, "Two-Stage Design Method for Enhanced Inductive Energy Transmission with Q-Constrained Planar Square Loops," *PLoS One*, vol. 11, no. 2, p. e0148808, Feb. 2016, doi: 10.1371/journal.pone.0148808.

[11] L. L. Pon, M. Himdi, S. K. A. Rahim, and C. Y. Leow, "Dual-Band Resonator Designs for Near-Field Wireless Energy Transfer Applications," in *Wireless Energy Transfer Technology*, InTech, 2019, p. 13.

[12] N. Inagaki, "Theory of Image Impedance Matching for Inductively Coupled Power Transfer Systems," *IEEE Trans. Microw. Theory Tech.*, vol. 62, no. 4, pp. 901–908, Apr. 2014, doi: 10.1109/TMTT.2014.2300033.

[13] M. L. Kung and K. H. Lin, "Enhanced analysis and design method of dual-band coil module for near-field wireless power transfer systems," *IEEE Trans. Microw. Theory Tech.*, vol. 63, no. 3, pp. 821–832, 2015, doi: 10.1109/TMTT.2015.2398415.

[14] T. Imura and Y. Hori, "Maximizing Air Gap and Efficiency of Magnetic Resonant Coupling for Wireless Power Transfer Using Equivalent Circuit and Neumann Formula," *IEEE Trans. Ind. Electron.*, vol. 58, no. 10, pp. 4746–4752, Oct. 2011, doi: 10.1109/TIE.2011.2112317.

[15] L. L. Pon, S. Kamal, A. Rahim, C. Y. Leow, and T. H. Chua, "Non-radiative wireless energy transfer with single layer dual-band printed spiral resonator," *Bull. Electr. Eng. Informatics*, vol. 8, no. 3, pp. 744–752, 2019, doi: 10.11591/eei.v8i3.1593.